*ICES Journal of Marine Science*, 2022, **79**, 2069–2083
DOI: 10.1093/icesjms/fsac138
Advance access publication date: 6 August 2022
**Original Article**

# Influence of near bottom fish distribution on the efficacy of a combined hydroacoustic video survey

**Leif K. Rasmuson *, Scott R. Marion, Stephanie A. Fields, Matthew T.O. Blume, Kelly A. Lawrence and Polly S. Rankin**

Marine Resources Program, Oregon Department of Fish and Wildlife, 2040 SE Marine Science Drive, Newport, OR 97365 , USA
* *Corresponding author: tel: 541-867-4741; e-mail:* leif.k.rasmuson@odfw.oregon.gov

Combining hydroacoustics and underwater video is an effective tool for generating fish population estimates. However, hydroacoustics cannot be used to differentiate fish from the seafloor within an area known as the acoustic dead zone. A common way to address this is to exclude data near the bottom. The effect of this exclusion zone on population estimates of nearshore semi-pelagic rockfish is unknown. This study explores the effect of a near bottom (0–1 m) exclusion zone by comparing ROV video data to data from a combined hydroacoustic and video method. Higher densities of semi-pelagic species (Black and Blue/Deacon Rockfish) were observed in the combined acoustic and video method, suggesting that most of the population resides above the exclusion zone. Demersal rockfish observed by the ROV did not contaminate acoustic data of semi-pelagic species, since they remained within the exclusion zone. Results demonstrate that extrapolation of school data into the exclusion zone provided a realistic correction to the acoustic data for Black Rockfish. Our work demonstrates that excluding the data within 1 m of the bottom does not negatively affect the ability of the combined video hydroacoustic method to sample semi-pelagic rockfish.

**Keywords:** acoustics; acoustic dead zone; Hydroacoustic surveys, rockfish, ROV, underwater camera.

## Introduction

Effective fishery management benefits from rigorous and systematic fisheries independent surveys to provide fish abundance estimates (Hilborn and Walters, 1992). Fisheries independent surveys can take many forms, including hook and line, trawl, video, and acoustic sampling techniques. Acoustic surveys are cost effective because large areas can be surveyed relatively quickly with minimal staff, but often need to be paired with another tool to provide species and length composition data (Misund, 1997; McClatchie *et al.*, 2000). These methods have proven effective for many pelagic and semi-pelagic stocks, as well as for stocks that occupy deep (depths >100 m) high-relief environments such as: Acadian Redfish (*Sebastes fasciatus*) and Orange Roughy (*Hoplostethus atlanticus*) (Kloser *et al.*, 2002; Gauthier and Rose, 2005). Although acoustic methods are well developed for species occupying deeper habitats, there has been limited research on the utilization of acoustics in shallow (<50 m depth) high-relief environments. For semi-pelagic species that spend some component of their time on or very near the bottom, differentiation of a fish's echo from that of the bottom is a difficulty for many acoustic systems (Ona and Mitson, 1996; Rasmuson, 2021).

Hydroacoustic surveys often refer to the area directly above the bottom as the acoustic dead zone, hereafter referred to as the dead zone (Ona and Mitson, 1996; Totland *et al.*, 2009; Kotwicki *et al.*, 2018). The dead zone is a region in which acoustic returns of fish overlap with returns from the seafloor. The thickness of this region is influenced by echosounder settings, water depth, and bottom relief. Unintended integration of the bottom signal into the fish signal, even if relatively small, can inflate a population estimate (Mello and Rose, 2009; Tušer *et al.*, 2013; Kotwicki *et al.*, 2018). Therefore, it is common to either extrapolate the above dead zone acoustic returns into the dead zone or exclude acoustic data near the bottom all together. The former assumes homogeneity in fish density and distribution, while the latter may result in underestimating the population, however, both require calculating the thickness of the dead zone to ensure these data are probably addressed (Mcquinn *et al.*, 2005). In shallow water, the mathematically calculated dead zone is thin relative to the depth of the water column (Ona and Mitson, 1996). Even so, for semi-pelagic fish occupying the region directly above the bottom, exclusion of near bottom fish could reduce the population estimate (Mcquinn *et al.*, 2005). Thus, in order to provide a corrected population estimate that includes the dead zone, some surveys have combined multiple survey tools that sample different regions of the water column to determine the fish density both above and within the dead zone (Kloser, 1996; Jones *et al.*, 2012; Kotwicki *et al.*, 2018).

Population estimates derived from acoustics require assigning acoustic observations to species, a process which is susceptible to error due to vertical segregation of both different species, and different sizes of individuals within the species (Stanley, 1999; McClatchie *et al.*, 2000; Gauthier and Rose, 2005). The potential for incorrect assignment of species is higher when vertical segregation occurs near the dead zone boundary. Therefore, employing sampling techniques both above and within the dead zone is necessary in order to assign inter- and intra-species vertical segregation (Jones *et al.*, 2012; Kotwicki *et al.*, 2018). In low-relief habitats, combining bottom and midwater trawls is an effective, albeit potentially destructive way to sample both above and within the dead zone. However, for semi-pelagic species that occupy high-relief habi-

**Received:** April 4, 2022. **Revised:** July 1, 2022. **Accepted:** July 5, 2022

tats, use of trawls is not feasible. Underwater cameras are proposed as an alternative tool to sample high-relief areas (Jones *et al.*, 2012), and by utilizing stereo camera technology, they are also able to provide fish lengths (Denney *et al.*, 2017).

Due in part to the large diversity and geographic range of the genus *Sebastes*, rockfish have been a pivotal species group to the development of combined video and hydroacoustic sampling methods. Early work showed acoustic sampling was effective for the continental shelf stocks of Yellowtail (*Sebastes flavidus*), and Widow Rockfish *(Sebastes entomelas*) (Stanley, 2000). In these studies, length, and species composition data came from midwater trawls. Examining deep water demersal rockfish, Jones *et al.* (2012) demonstrated that deep untrawlable rocky reefs are important rockfish habitats, that need to be surveyed and included in population estimates. Jones *et al.* (2012) compared the utility of using a stereo drop camera to estimate the population size of rockfish in the dead zone, to the extrapolation method of Ona and Mitson (1996). They demonstrated that the dead zone contained many of their focal species. Nearshore semi-pelagic rockfish are under-surveyed, even though species like Black Rockfish (*Sebastes melanops*) are the primary catch of the recreational and commercial nearshore fleets in Oregon. (Tschersich, 2015; Boettner and Burton, 1990) demonstrated that acoustics are a viable tool for Black Rockfish surveys. However, Tserchich (2015) utilized only echo counting (not echo integration, as is necessary for large–dense schools) and therefore did not require length composition. Boettner and Burton (1990) obtained length samples using a midwater trawl, which while effective, is not suitable in high-relief nearshore habitat. Thus, Rasmuson *et al.* (2021) combined a suspended stereo camera system with hydroacoustics to estimate nearshore semi-pelagic rockfish densities. They suggested that this combination is an effective and efficient way to survey semi-pelagic rockfish densities in shallow, high-relief areas. However, near-bottom was excluded when analysing the acoustic data and the effect of that procedure was not fully examined, further the relative contribution of other rockfish species to the signal in the acoustic data were not considered.

In the present study, our goal was to estimate the influence of near bottom fish on the combined acoustic–visual survey designed to provide a population estimate for three semi-pelagic species—Black, Blue (*Sebastes mystinus*), and Deacon Rockfish *(Sebastes diaconus*). Specifically, we determined what portion of the population of these three species occurred within the area of the water column directly above the bottom that is not captured by our acoustic system, an area we refer to as the exclusion zone, as well as whether or not, demersal rockfish affected population estimates of the three target semi-pelagic species. To answer these questions, we compared acoustic swath data and point estimates from our suspended camera with co-located benthic-oriented video data from remotely operated vehicle (ROV) belt transects conducted immediately following the acoustic sampling. We assessed whether the survey tool observations were associated by testing if (1) the ROV and suspended camera generate similar size distribution estimates, and (2) the acoustic-visual sampling followed by ROV sampling was successful in detecting spatially consistent concentrations of fish across the reef. Assuming associations between tools were found, we examined how these data could be used to provide density corrections to the exclusion zone. Finally, for each species/species group, we compared total density estimates from each tool as a proxy for how much of each population was above (available to acoustics) vs. within (available to ROV) the exclusion zone.

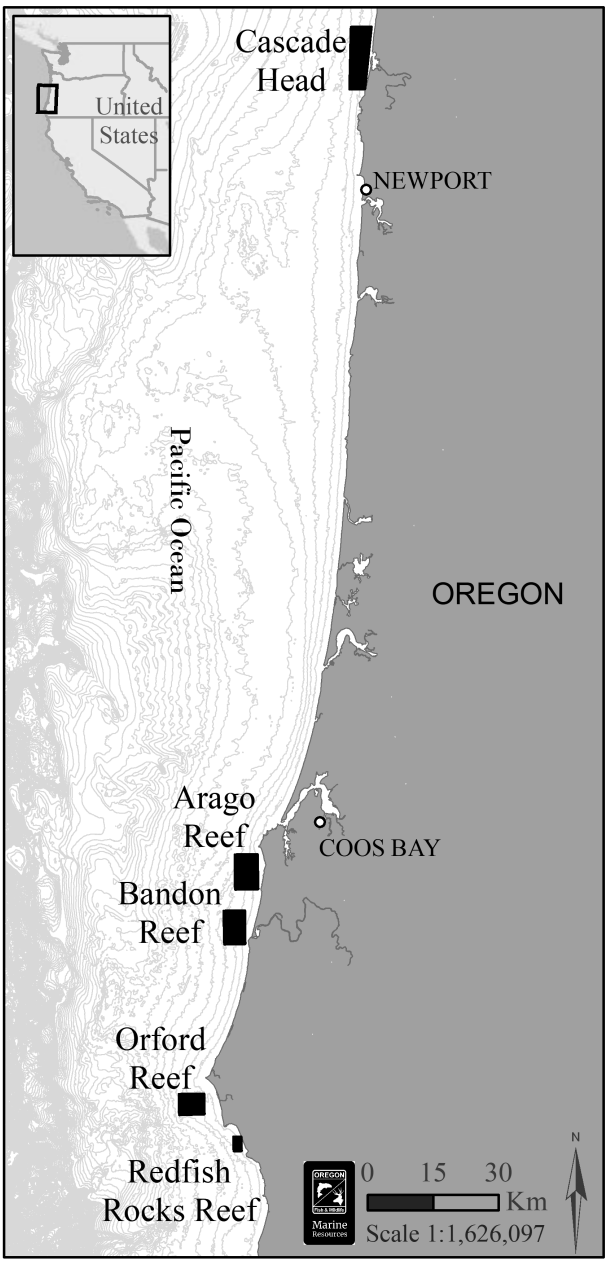


**Figure 1.** Map of study areas along Oregon coast. Black boxes denote the approximate locations of each reef. Cascade Head was sampled in May of 2018, whereas all other reefs were sampled in September of 2018.

## Material and methods

### Field work

Acoustic and visual surveys of shallow, nearshore rocky reefs were conducted in the spring and fall of 2018 (Figure 1). Surveys were conducted on five reefs spread over 250 km along the south/central Oregon coast: Cascade Head (44.88°N, 124.09°W), Cape Arago (43.28°N, 124.46°W), Bandon (43.17°N, 124.48°W), Orford Reef (42.77°N, 124.60°W), and Redfish Rocks (42.70°N, 124.48°W). At each reef, transects were randomly placed within the known area of rocky reef, defined as mapped areas having cobble or larger sub-

strates, between 20 and 50 m depth. These survey boundaries reflected the shallow end of the ROV's safe working range and the deep end of the expected distribution of Black Rockfish (Love *et al.*, 2002). All transects were oriented in a NW–SE direction, anticipating the likely direction of predominant winds and waves. Transects conducted in the spring were 300 m in length, and in the fall transects were lengthened to 500 m. Transects were conducted from 1 h after sunrise to 1 h before sunset, as previous work has shown that species are sufficiently above the bottom to be available to acoustics during this time (Rasmuson, 2021).

### Acoustics and BASSCam

Except for Cascade Head, surveys were conducted aboard a 15.3 m charter passenger fishing vessel. At Cascade Head, surveys were conducted aboard a 7.6 m aluminum vessel. Operations and acoustic settings were the same on both vessels. Transects were first ensonified using a BioSonics 200 kHz split beam DT-X transducer with a beam width of 6.9°. Acoustic data were collected using a ping rate of 5 pings $s^{-1}$ and a pulse duration of 0.3 ms. The transducer was calibrated at the BioSonics factory before and after the survey. The three largest fish schools identified while ensonifying the transect were sampled with the camera system following the transect completion. In the event no schools were identified from the acoustics; rugose habitat regions were targeted for camera deployments. Camera drops occurred within 1 h of completion of the transect, though most occurred within 20 min.

Camera deployments were conducted using the benthically anchored suspended stereo camera (BASSCam) described by Rasmuson *et al.* (2021). Briefly, the system floats 2-m off bottom and consist of a stereo pair of forward-facing GoPro Hero4 Black cameras, and a single GoPro Hero4 Black camera facing downward at an angle of 22° below horizontal (see Figure S4 in the online supplement for a diagram of the viewed areas by the forward and downward-facing cameras). The forward-facing cameras were spaced 39.4-cm apart from one another and angled inwards at 8°. The three cameras were illuminated by Big Blue LED dive lights, four 9 000 lumen lights looking forward and two 7 500 lumen lights looking down. Unlike in previous work, there was no live video feed to the surface. A total of 2-min deployments were conducted; previous work showed a 2-min deployment was sufficient to provide accurate length and count data (Rasmuson unpublished), and that the BASSCam has little to no effect on the behaviour of schooling fish (Rasmuson *et al.*, 2021).

### ROV

ROV surveys were conducted using a Deep Ocean Engineering Phantom HD2 + 2 ROV. The primary fish abundance data were gathered using a high-definition video camera (Blackmagic Micro Cinema with an 8 mm wide-angle lens) at an angle of 30° below horizontal, with parallel red lasers providing a 10 cm scale reference. Two Nuytco 200-watt H.M.I. lights provided illumination for the forward-looking camera. Altitude above the seafloor was recorded with two ranging altimeters, one mounted on the forward-looking camera housing, and one mounted vertically. A second Blackmagic camera, paired with a pair of 10 cm scaling lasers, was pointed straight down in front of the ROV for navigation purposes, but these data were not used in the present study. Two down-facing SeaLite Matrix LED lights illuminated the substrate for the downward-facing camera. A calibrated forward-facing stereo video system provided sub-centimeter accurate measurements of fish length and fish height off bottom. Two GoPro Hero4 Black cameras were mounted in custom flat-port housings (Sexton Corporation) on the front of the ROV spaced 47-cm apart from one another and angled inwards at 6°.

The ROV was navigated using an acoustic tracking system (ORE Offshore Trackpoint III), with raw ROV positions determined at 4 s intervals and subsequently smoothed to minimize any positional artifacts. This equipment and processing typically yields a positional accuracy of ± 4 m. ROV transects were conducted between 0.5 and 1.5 m above the bottom at a target speed of 0.5–1 knot, resulting in a typical transect width of 2–5 m. ROV sampling occurred within ∼1 h of the acoustic transect for half of all transects, and within 2 h for 90% of all transects.

## Data processing

### BASSCam

BASSCam video was reviewed using EventMeasure software by SeaGIS followed methods described by Rasmuson *et al.* (2021). In each video, five randomly selected frames were chosen and all fish in each frame were identified to the lowest taxonomic level possible. Fish were counted and the observation coded as occurring in either the forward or downward-facing camera. Fish in the forward cameras were measured only if they were oriented approximately perpendicular to the cameras.

The focus of this study was nearshore semi-pelagic rockfish (Black, Blue, and Deacon Rockfish). Blue Rockfish and Deacon Rockfish can be difficult to distinguish from one another in the video so were considered as a single species group. All other observed semi-pelagic species (Yellowtail, Widow, Puget Sound (*Sebastes emphaeus*), and Canary Rockfish (*Sebastes pinniger*) were aggregated into a functional group called non-focal semi-pelagic rockfish. Remaining rockfish species observed were classified into a functional group called demersal rockfish (**Table 1**). Juvenile rockfish were excluded from analysis because of discrepancies in how the two video tools identified juvenile rockfish. Differences were associated with, if juveniles were coded by species or as unidentified, and if the unidentified were specific to juveniles or all age groups together. All other observed species and functional groups were excluded from additional analysis.

### Acoustics

Processing of the acoustic data, including algorithm settings, followed the methods outlined by Rasmuson *et al.* (2021). Additionally, an example echogram and a description of the acoustic review process are presented in Rasmuson *et al.* (2021). In the present study, to exclude the near-bottom dead zone, subtidal aquatic vegetation, and to allow for comparison with the ROV, acoustic data within 1 m of the bottom was excluded. All analyses were conducted in Echoview version 11. Acoustic data were analysed using both echo integration and echo counting. Portions of echograms were assigned to each analytical method using the Sawada index and the ratio of multiple echoes (Sawada *et al.*, 1993). Both indices independently identify regions of the echogram where fish densities are so high that they cannot be analysed using echo counting and are therefore analysed using echo integration. In regions analysed with echo integration, the school detection algorithm identified schools that had been smoothed with a median 3 × 3 filter. The school detection algorithm applies user defined thresholds and algorithms to identify fish schools in

**Table 1.** Fish species and counts observed by the ROV and BASSCam.

| Common name | Scientific name | Species/Species group | ROV | BASS |
|---|---|---|---|---|
| Black rockfish | *S. melanops* | Black | 1 770 | 1 111 |
| Blue rockfish | *S. mystinus* | Blue/Deacon | 25 | NA |
| Blue/Deacon rockfish | *S. mystinus/diaconus* | Blue/Deacon | 3 022 | 2 325 |
| Canary rockfish | *S. pinniger* | Non-focal semi-pelagic | 689 | 95 |
| China rockfish | *Sebastes nebulosus* | Demersal | 211 | 8 |
| Copper rockfish | *Sebastes carnatus* | Demersal | 44 | 8 |
| Deacon rockfish | *Sebastes diaconus* | Blue/Deacon | 2 980 | NA |
| Puget Sound rockfish | *S. emphaeus* | Demersal | 54 | 0 |
| Quillback rockfish | *Sebastes maliger* | Demersal | 338 | 9 |
| Rosethorn rockfish | *Sebastes helvomaculatus* | Demersal | 25 | 0 |
| Tiger rockfish | *Sebastes nigrocinctus* | Demersal | 14 | 0 |
| Vermilion rockfish | *Sebastes miniatus* | Demersal | 81 | 11 |
| Widow rockfish | *S. entomelas* | Non-focal semi-pelagic | 88 | 6 |
| Yelloweye rockfish | *Sebastes ruberrimus* | Demersal | 142 | 17 |
| Yellowtail rockfish | *S. flavidus* | Non-Focal Semi-pelagic | 183 | 38 |

BASSCam counts are from one randomly selected observation frame per deployment.

the echogram (Nero and Magnuson, 1989; Barange, 1994; Haralabous, 1996). The regions defined as schools were then visually checked for accuracy and edited as needed. To convert the acoustic backscattering data from fish schools into densities, the *Sebastes* average target strength to length relationship described by Rasmuson *et al.* (2021) was used. The same methods were used to derive fish densities. Length data were provided by the BASSCam in 1 cm length bins and scaled by species/species groups.

After school detections were completed, the echogram was examined visually to define regions for echo counting. In these regions, an Echoview's single target algorithm was applied to identify individual fish echoes. Considering it is common for multiple acoustic targets to represent a single observed fish, we then used an Echoview's fish tracking algorithm (Balk and Lindem, 2000; ICES, 2000) to identify instances where multiple echoes were attributable to only a single fish and converted them into a single fish observation (known as a fish track). Individual fish echoes were converted to density by taking into account its depth in the water column and the area surveyed by the acoustic beam at that depth (Tschersich, 2015). Densities of fish echoes were summed to generate a total density per transect.

### ROV

Digital video files from the main forward-oblique camera were reviewed by a highly trained technician, and time-stamped fish observations were geolocated by merging with time-stamped ROV navigation records.

A trapezoidal screen overlay extending from the full width at the bottom of the screen, tapering to 80% of screen width at 80% of screen height, was used to exclude areas too distant or marginal to allow reliable fish identification. Sections of video were excluded if the reviewer estimated that a 20 cm fish could be obscured in more than 20% of the review frame (e.g. due to poor visibility, terrain obstructions, or ROV maneuvering), or if the ROV was not making relatively linear forward progress. For the remaining valid portions of transects, subsequently referred to as "non-gap" data, fish were identified to species, where possible, for 24 target species and otherwise were recorded in higher-level taxonomic groupings.

Using the scaling laser contact points with the seafloor and predetermined camera calibrations, transect width was derived at 30 s intervals then interpolated for each 1 s interval. Surveyed area for each 1 s interval was calculated by multiplying the transect width by the along-transect distance. Fish densities were generated from fish counts by dividing non-gap fish counts by the non-gap surveyed area.

ROV derived stereo imagery was reviewed using an EventMeasure. Total length was measured for each appropriately positioned and oriented fish. Fish height off bottom was measured by estimating and measuring to the nearest visible rock, when both a distinguishable feature on the bottom and a fish were visible in a stereo image. Fish visibly resting on the seafloor were assigned a height of 0.

## Statistical analysis

All statistical analyses were conducted using R version 4.1.2 Bird Hippie (R Core Team, 2020).

### Length data comparison

To determine if the ROV and BASSCam observed fish of similar lengths, we compared the length distributions of Black and Blue/Deacon Rockfish between the two tools at each reef. Plots were developed using scaled densities and statistically compared using a Kolmogorov–Smirnoff test.

We also used the selectivity ratio defined by Kotwicki *et al.* (2017) to determine if either tool observed a greater proportion of Black or Blue/Deacon Rockfish of a certain size class. The selectivity ratio was calculated using the SCMM approach and the mgcv package in R (Wood, 2006, 2011). Lengths were aggregated into 2 cm bins and a two-stage resampling method with 1 000 bootstrap resamples was applied.

### Spatial correspondence among tools

To assess the validity of the assumption that the two sampling tools were sampling a similar spatial distribution of fish along the reef (i.e. that schools did not move substantially between observation by the acoustics and observation by the ROV, and that the proximity of the ROV transect to the acoustic transect was sufficient), we spatially compared the fish densities observed by the acoustics with those observed by the ROV along each transect. Transects were divided into segments, approximately 50 m in length. To avoid splitting schools at the segment boundaries, we adjusted the segment split points by examining local acoustically-estimated fish density and moving the split points to a local minimum. Resultant segments had variable lengths, with 90% of segments falling between

42 and 63 m. Data were excluded where the ROV and acoustic transects were separated by more than 10 m, and entire segments were excluded if the total remaining area sampled by ROV was less than 25 $m^2$. This resulted in a data reduction of ~10%.

To examine the spatial agreement in the presence and absence of fish between the ROV and acoustics, we generated a confusion matrix (Visa *et al.*, 2011). The confusion matrices were generated for the Black, Blue/Deacon, non-focal semi-pelagic, and demersal rockfish categories separately. Data from Cascade Head were excluded from this analysis due to the extreme low numbers of fish observed by both tools. Using these confusion matrices, we derived two indices to assess the agreement between our tools. Accuracy, an index of relative agreement between the tools (Allouche *et al.*, 2006), was calculated as:

$$\text{Accuracy} = \frac{RA + N}{RA + N + R + A}, \quad (1)$$

where $R$ denotes only the ROV detected fish, $A$ only the acoustics detected fish, $RA$ both tools detected fish, and $N$ neither tool detected fish. Sensitivity of the was calculated as:

$$Sensitivity = \frac{RA}{RA + A}, \quad (2)$$

where $RA$ and $A$ are defined as above.

In addition to assessing the correspondence between the acoustics and ROV in segment–scale presence/absence, we also calculated the Pearson's correlation coefficient between the segment–scale densities from the two tools.

### Exclusion zone densities within fish schools

The goal of this analytical component was to determine if the BASSCam's downward-facing camera accurately accounted for fish in the exclusion zone in the acoustics. Determining how proportions of fish differed above and below the exclusion zone informed whether there is a need for a numerical density correction above the exclusion zone when multiplying data downwards into the exclusion zone. Analyses were conducted on BASSCam and ROV data, no acoustics were included in this analysis. BASSCam drops were excluded if there was no ROV data collected within 20 m of the deployment. This resulted in no demersal rockfish observations for the BASSCam. We modelled the proportion of fish above the exclusion zone (thereby standardizing differences in viewed areas between tools), using the explanatory variables: tool, functional species/species group, and reef. Data from Cascade Head were excluded from this analysis due to the extremely low numbers of fish observed by both tools.

ROV count data within 20 m of the BASSCam drop were summed to provide total counts above and within the exclusion zone for each transect. The distance of fish off bottom measured in the ROV video was determined using the forward-facing stereo cameras. Proportion of fish located above the exclusion zone was then calculated as the number above 1 m divided by the total number measured.

BASSCam volume was calculated from the area viewed by the forward cameras using a fixed maximum range across all transects. The fixed maximum range was the average of each transects maximum range (i.e. the distance to the furthest fish viewed in the three BASSCam drops). Maximum range did not differ greatly ($2.8 \pm 0.4$ m), so a single value was used for all transects. In all instances, the downward camera's maximum viewed distance was the bottom, so the volume for the downward-facing camera was calculated using the known height of the camera off bottom and assuming a flat bottom. The volume of water viewed by the downward-facing camera was 88% of the volume viewed by the forward camera. Therefore, fish counts from the downward-facing camera were first divided by 0.88 to standardize counts between the two volumes. Then, as the goal was to determine how many fish were in the exclusion zone, we also determined that 78% of the observed volume observed by the downward-facing camera occurred within the exclusion zone (from 0 to 1 m off bottom). Therefore, a correction was applied to the standardized counts from the downward-facing camera by multiplying them by 0.78 to represent only what was counted within the exclusion zone. All fish viewed in the forward camera were considered above the exclusion zone. We made this assumption, since in most instances, only the area above 1 m was viewed due to poor visibility. The proportion of fish above the exclusion zone was generated for the BASSCam by dividing the number of fish in the forward camera by the number in the forward plus the corrected number from downward-facing camera.

We modelled the proportion of fish above the exclusion zone using a binomial distribution. Modelling required summing counts across the three BASSCam deployments per transect, and analysing proportions, instead of raw counts. Models were fit using the *glm* function in the base *stats* package, using the potential covariates: Species/species group/functional group, Reef, and Camera. All possible model iterations were fit, and a best-fit model was selected using the Akaike Information Criterion (AIC). Relative strength of model selection was assessed using both Akaike weights and log likelihood.

### Fish densities outside schools

In a hypothetical survey utilizing only acoustics and BASSCam, data on fish abundance and composition in the exclusion zone would come only from BASSCam drops, which, in the current study only targeted schools. Therefore, data regarding fish in the exclusion zone but away from schools are missing from the BASSCam and acoustics. To assess whether this away-from-schools near-bottom data was influential to overall conclusions about semi-pelagic fish abundance, background fish density (defined here as the density of fish outside fish schools in the exclusion zone) was calculated from ROV data. First, the location of fish schools and school edges were defined from the acoustic data. Fish densities of each species/species group in the ROV data were then calculated in concentric 5 m increments from the school edge to a distance of 50 m.

To determine at what distance from a school background fish densities were observed, we used generalized additive models. Each species/species group was modelled independently. Response data were fish counts per 5 m distance bin. Explanatory variables were distance from school and reef. Fish count was modelled with a negative binomial distribution. Viewed area per increment was provided as a model offset. The best fit models were selected from all possible model formulations that included variables reef and distance, using AIC and relative strength of model selection, assessed using Akaike weights and log likelihood. The resulting GAM plots were used to visually identify the distance at which background density occurred. We calculated the mean ("background") density in the exclusion zone from all ROV data at

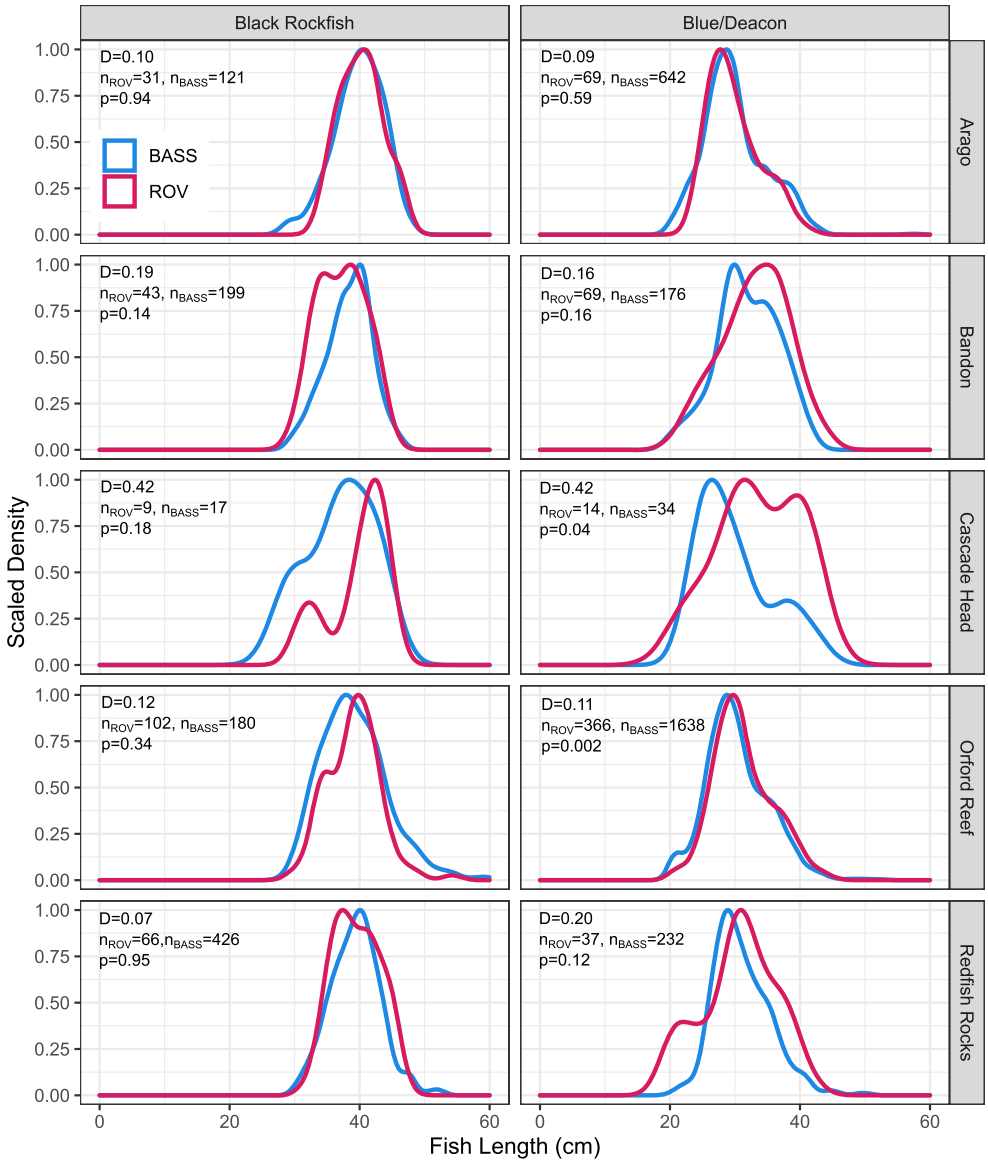


**Figure 2.** Scaled density plots of length distributions for the 3 target species/species groups at each reef. Values in the plot represent the results of a statistical comparison of the 2 densities using a Kolmogorov–Smirnov test. *D* is the Kolmogorov–Smirnov test statistic.

distances from schools greater than the selected threshold distance.

### Density estimate

Density estimates from acoustic data were generated from the echo integration and echo counting data (see section 2.2.2) and were created for each species/species group separately. Densities from both methods were summed for each transect and mean transect density calculated for each species/species group at each reef.

ROV fish count data from the main camera were used to generate mean densities per species/species group per reef. For each transect, each species/species group's density was calculated as the total fish count within non-gap portions of the transect divided by the non-gap surveyed area. The reef-level mean density was calculated as the weighted mean +/- weighted *SD* of the transect densities, using the non-usable survey area for each transect as the weight.

## Results

A total of 157 transects were sampled with both the ROV and the acoustics/BASSCam survey methods (see online supplement for maps of each reefs transects). The two video tools observed 3 species or species groups, and 38 656 fish were counted; of these, 13 294 individual fish from 16 species or species groups were used in additional analyses (**Table 1**). The ROV, with a far greater area surveyed, observed more species and individuals than the BASSCam. In the acoustic data, 340 schools of fish and 1 403 fish tracks were identified.

### Length data comparison

Length distributions between the two tools at each reef were similar (Figure 2). Exceptions were Blue/Deacon Rockfish at Cascade Head and Orford Reef. Although there were some statistical differences among these species and locations, their overall distributions were visually quite similar.

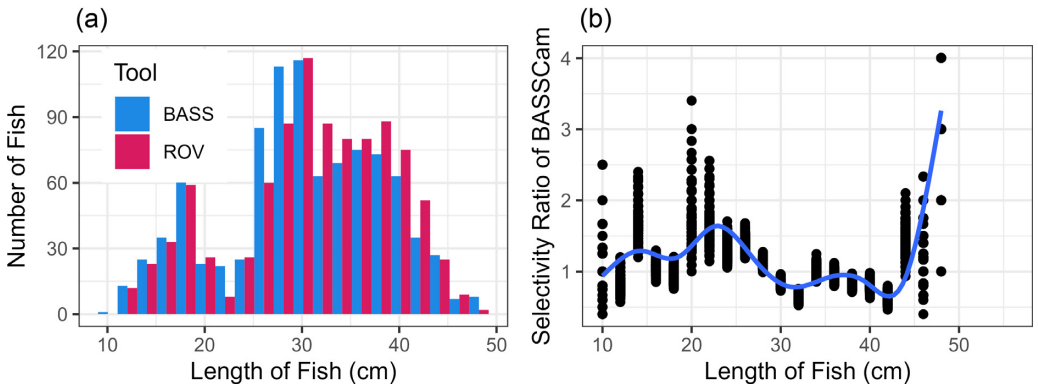


**Figure 3.** Number of fish measured by length (a) and selectivity of the BASSCam relative to the ROV for Black and Blue/Deacon Rockfish (b). For selectivity, values above 1 indicate greater selection by the BASSCam and values less than 1 indicate greater selection by the ROV. Black dots denote each estimate of selectivity from 1 000 sampling iterations and the blue line denotes the estimate of selectivity from a generalized additive model of selectivity vs. length.

Length selectivity analysis for Black and Blue/Deacon Rockfish demonstrated the BASSCam observed slightly more fish with lengths of 12–30 cm than the ROV, and the ROV observed more fish at lengths >30 cm (Figure 3). However, the selectivity ratio was very small (average of 1.07), suggesting that although evidence of selectivity in length existed, the magnitude of the effect was very small.

### Spatial correspondence among tools

In general, there was spatial overlap in where the ROV and the acoustics/BASSCam observed fish. The accuracy calculated from the presence/absence confusion matrix was 72% for Black Rockfish, 77% for Blue/Deacon Rockfish, 71% for non-focal semi-pelagic rockfish, and 65% for demersal rockfish. The sensitivity was 42% for Black Rockfish, 53% for Blue/Deacon Rockfish, 39% for non-focal semi-pelagic rockfish, and 37% for demersal rockfish. Density estimates for Black Rockfish and Blue/Deacon Rockfish were moderately well correlated between tools ($r = 0.58$, $p < 0.001$ for both groups, Figure 4). For the non-focal semi-pelagic and demersal rockfish, density correlations were non-significant, and poor, respectively (Figure 4).

### Exclusion zone densities within fish schools

Our best fit model included an interaction between species/species group and video tool (**Table 2**, see online supplement Table S1 for summary of best fit model). The next best fit models had AIC values ~ 15 units higher than the best fit model, suggesting strong consensus in model selection. This was corroborated by Akaike weight and log likelihood values of 1. The BASSCam observed a higher proportion of fish above the exclusion zone than the ROV for all semi-pelagic functional groups (Figure 5). The ROV observed few demersal rockfish above the exclusion zone. Blue/Deacon Rockfish were seen primarily above the exclusion zone in both tools.

### Fish densities outside schools

Our best fit model of fish density in relation to the distance from school included an interaction between reef and distance, with reef as an independent factor (**Table 3**, see online supplement for summary of best fit models and plots of raw data). The best fit model for each species/species group, except demersals, was well supported (high Akaike weights). Unsurprisingly, models of demersals had relatively poor fits, as trends in demersal rockfish density were not expected to be influenced by the locations of schooling fish. Examination of the GAM smooths suggested that excluding the area within 35 m of fish schools would result in a reasonably conservative estimate of background (non-school) fish density (i.e. likely to exclude all influence of schools), for Black and Blue/Deacon rockfish (Figure 6). Background densities were calculated for each species/species group using all data from the region greater than 35 m from school edges (**Table 4**).

### Density estimate

The total reef density estimates of Black and Blue/Deacon Rockfish were higher when derived from the acoustics/BASSCam than from the ROV (Figure 7), which was expected, due to the ROV only viewing the bottom component of the vertical distribution of the schooling species. Black Rockfish were 5.7 times more prevalent in the video–hydroacoustic data than in the ROV data, and Blue/Deacon Rockfish were 9.7 times more prevalent in the video–hydroacoustics than in the ROV data. However, an extremely high-density of Blue/Deacon Rockfish were observed in the video–hydroacoustics at Cape Arago, and if these data are excluded, Blue/Deacons were only 2.9 time more prevalent in the video–hydroacoustics than the ROV data. Conversely, demersal rockfish were 16.5 times more prevalent in the ROV data than the video-hydroacoustics, again consistent with the on-bottom distribution of these solitary species. Non-focal semi-pelagic rockfishes were 1.6 times more prevalent in the video–hydroacoustics than ROV, but it is worth noting the densities of this species group were extremely low and variable compared to the other species groups. The coefficient of variation was quite high for both tools (**Table 5**).

## Discussion

In this study, we set out to assess the relative effect of applying a near-bottom exclusion zone (area above the bottom excluded to account for the near-bottom dead zone) to an acoustic survey of Oregon's nearshore semi-pelagic rockfish. We paired a combined hydroacoustic and underwater video sampling method (BASSCam) with ROV video sampling to

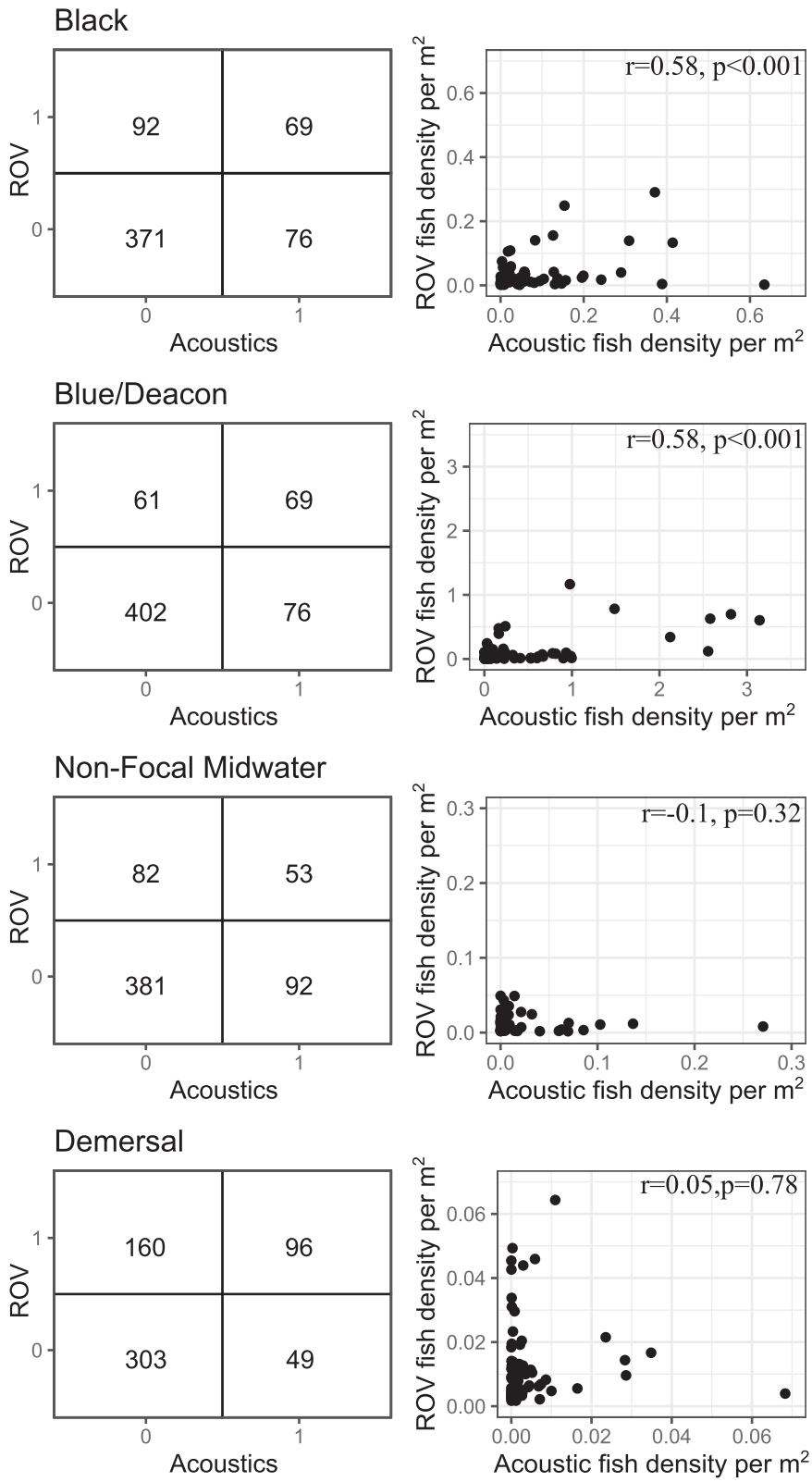


**Figure 4.** Confusion matrices of fish presence/absence by transect segment (left) and correlation of segment fish densities (right, with Pearson's correlation statistics) among tools (Acoustics vs. ROV) for each species group. In the confusion matrices 1 denotes fish were observed and 0 denotes no fish were observed.

**Table 2.** Relative model fit variables and model selection criteria (Delta AIC, Log Likelihood and Akaike Weight) for every model formulation used to compare the proportion of fish in the exclusion zone among tools.

| Formula | Delta AIC | Log likelihood | Akaike weight |
|---|---|---|---|
| Camera∗Species∗Reef | 26.09 | 0 | 0 |
| Species∗Reef | 29.74 | 0 | 0 |
| Camera∗Reef | 41.86 | 0 | 0 |
| Camera∗Species | 0 | 1.00 | 1.00 |
| Species | 16.22 | 0 | 0 |
| Reef | 80.72 | 0 | 0 |
| Camera | 34.31 | 0 | 0 |
| 1 | 79.67 | 0 | 0 |

Delta AIC, Log Likelihood and Akaike weight are used to assess the quality of model fits. A Delta AIC of 0 denotes the best fit model. A log likelihood and Akaike weight of 1 denotes a model with strong support. Reef: Study reef; Camera: ROV vs. BASSCam; Species: species/species group (Table 1). The response variable was the proportion of fish within the exclusion zone out of the total number counted and was modelled using GLMs with a binomial distribution.

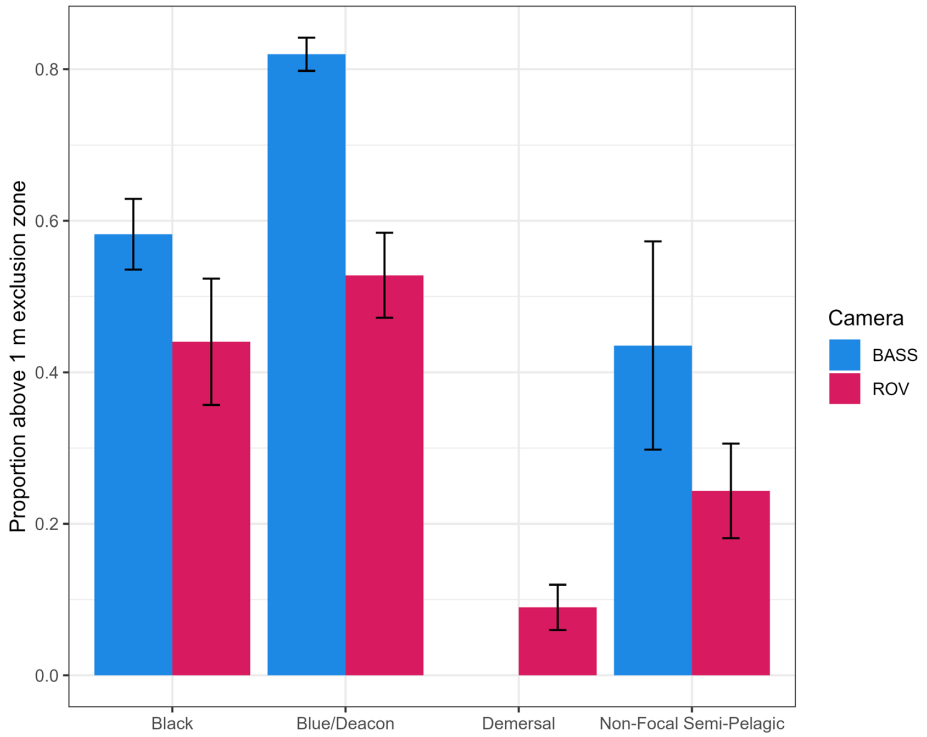


**Figure 5.** Average proportion (± *SD*) of fish observed above the exclusion zone (0–1 m) across all reefs by each tool, for each of the 4 species/species groups. No demersal fish were observed by the BASSCam in locations with collocated ROV data. Model selection suggested there was no effect of reef (see Table 2).

determine the relative contribution of the exclusion zone to the overall abundance estimate. However, we first had to assess whether the observations from each tool were similar to one another. We found that the length distributions of our target species/species groups differed minimally between the tools, and there was little evidence of size selectivity between tools (Kotwicki *et al.*, 2017). Further, there was good spatial coherence in the observations between our two tools, and the densities of observed fish were well correlated for the schooling semi-pelagic fish species targeted by this study. Based on these findings, we conclude, that by comparing these two survey methods we were able to accurately assess the relative importance of fish in the exclusion zone in an acoustic-based abundance estimate for semi-pelagic rockfish. We found that overall, a relatively small proportion of our focal semi-pelagic rockfish were within the exclusion zone, suggesting the combined hydroacoustic suspended camera survey is able to accurately observe most of our focal species. The findings reported in this study suggest the BASSCam approach could correct for fish within the exclusion zone that are missed by the acoustics and support further investigation into the use of a combined hydroacoustic video methodology in future large-scale surveys. However, our results also show that longer acoustic transects are necessary in order to reduce the variability in density estimates.

Different video sampling tools, especially moving platforms, inherently have the potential to affect fish behaviour. In this study, the ROV may elicit behavioural responses due to movement, noise, and artificial light of the tool. The BASSCam may elicit behavioural responses due to lights, structure in the water column, and bottom disturbance at the time of deployment. A quantitative assessment of how our two video sampling devices affected fish behaviour was not possible within the scope of this study. Previous work has shown that there is little effect of the BASSCam on fish behaviour (Rasmuson *et al.*, 2021). Further, during the review of many hours of video

**Table 3.** Delta AIC, Log likelihood, and Akaike weight values for every potential model formulation assessing the relationship between ROV-derived density and distance from the edge of each acoustically-detected school.

| Black | | | |
|---|---|---|---|
| **Formula** | **Delta AIC** | **Log likelihood** | **Akaike weight** |
| Distance∗Reef + Reef | 0 | 1.00 | 0.92 |
| Distance∗Reef | 4.84 | 0.09 | 0.08 |
| Distance + Reef | 13.99 | 0 | 0 |
| Distance | 38.29 | 0 | 0 |
| Reef | 42.48 | 0 | 0 |
| ~1 | 71.71 | 0 | 0 |
| **Blue/Deacon** | | | |
| **Formula** | **Delta AIC** | **Log likelihood** | **Akaike weight** |
| Distance∗Reef + Reef | 0 | 1.00 | 1.00 |
| Distance∗Reef | 44.96 | 0 | 0 |
| Distance + Reef | 10.83 | 0 | 0 |
| Distance | 43.26 | 0 | 0 |
| Reef | 26.85 | 0 | 0 |
| ~1 | 53.23 | 0 | 0 |
| **Demersal** | | | |
| **Formula** | **Delta AIC** | **Log Likelihood** | **Akaike Weight** |
| Distance∗Reef + Reef | 0 | 1.00 | 0.47 |
| Distance∗Reef | 1.62 | 0.44 | 0.21 |
| Distance + Reef | 3.65 | 0.16 | 0.08 |
| Distance | 2.08 | 0.35 | 0.17 |
| Reef | 5.97 | 0.05 | 0.02 |
| ~1 | 4.53 | 0.10 | 0.05 |
| **Non-focal semi-pelagic** | | | |
| **Formula** | **Delta AIC** | **Log likelihood** | **Akaike weight** |
| Distance∗Reef + Reef | 0 | 1.00 | 1.00 |
| Distance∗Reef | 10.96 | 0 | 0 |
| Distance + Reef | 14.49 | 0 | 0 |
| Distance | 18.63 | 0 | 0 |
| Reef | 21.89 | 0 | 0 |
| ~1 | 26.74 | 0 | 0 |

Delta AIC, Log likelihood, and Akaike weight are used to assess the quality of model fits. A Delta AIC of 0 denotes the best fit model. A log likelihood and Akaike weight of 1 denotes a model with strong support. Distance: distance from the edge of each fish school; Reef: study reef.

no systematic behavioural response to either camera platform was observed. Specifically, none of the species entered the field of view of the ROV in a manner that suggested either approach toward or flight from the device. Fish also did not appreciably change their height off bottom in response to the device.

Quantitative assessments of behavioural interaction of reef fish with sampling platforms can be exceedingly complex (Somerton *et al.*, 2017; Garner *et al.*, 2022) and species-specific behaviours (gear approach and gear avoidance) should be anticipated (Stoner *et al.*, 2008). Thus, extrapolating results from other species in different regions is not advised. Studying the *Sebastes* genus, Ryer *et al.* (2009) assessed simulated underwater vehicle lighting on behaviour of Black and Blue Rockfish. They found fish avoided approaching light, but that response was drastically reduced in high ambient light conditions. Our study was conducted in shallow water (<50 m) during daylight, suggesting high ambient light and a potentially lower risk of artificial light avoidance. Laidig *et al.* (2013) assessed movement of rockfish in California in response to an approaching ROV, but their study was much deeper (70–400 m), so the ambient lighting was much less than in our study, and neither Black Rockfish nor Deacon Rockfish were assessed. As such, although some studies have been conducted on the species of interest to this paper, further work is necessary to fully quantify behavioural responses to survey tools.

The dead zone has the potential to greatly influence the population estimates of species surveyed with hydroacoustics (Ona and Mitson, 1996). A common way to correct acoustic data is to extrapolate the acoustic backscattering data from above the exclusion zone into the exclusion zone (Kloser, 1996). While this method is often applied without validating the assumption of a consistent density, here we tested that an assumption by comparing the proportions of fish observed above and within the exclusion zone, and were able to confidently state that a linear extrapolation into the exclusion zone would provide a realistic correction to the acoustic data for Black Rockfish. The two video tools (ROV and BASSCam) found the proportion of Black Rockfish was only minimally different above and within the exclusion zone. In contrast, Blue/Deacon Rockfish were much more prevalent just above the exclusion zone than within it, so simple extrapolation of above-exclusion-zone densities from video would erroneously inflate a density estimate (and therefore the corresponding total abundance estimate) for this species. Our data suggest that either 1:1 extrapolation of acoustic data from above the exclusion zone into the exclusion zone, or an inclusion of a density estimate from the BASSCam could be used for Black Rockfish. However, for Blue/Deacon Rockfish an acoustic extrapolation would need to be reduced to account for the greater abundance above the exclusion zone suggesting a density estimate from the BASSCam may be more suitable.

Although our data suggest the BASSCam's downward-facing camera provides adequate data for correcting fish schools by multiplying their acoustic signature from above the

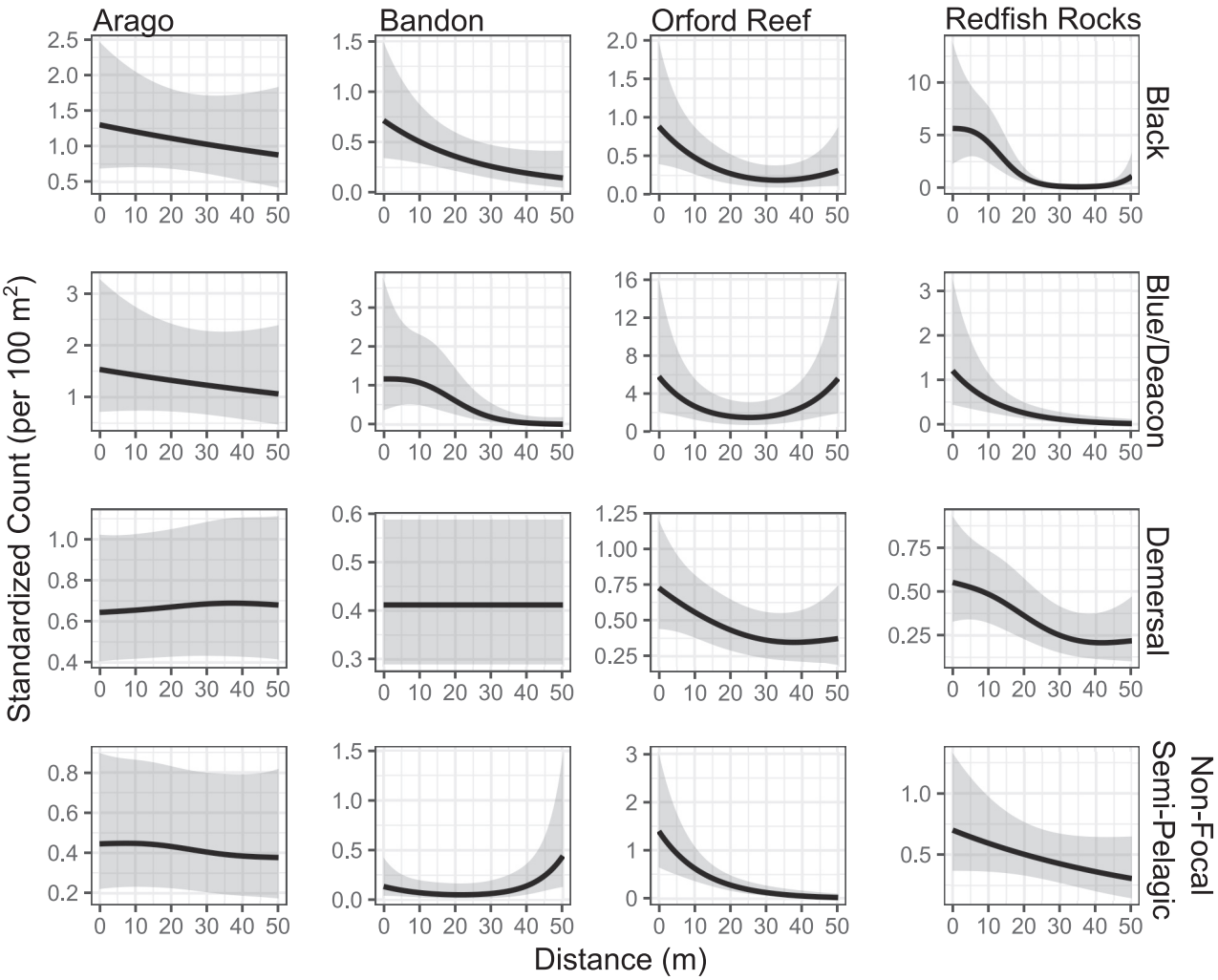


**Figure 6.** Generalized additive models relating the number of fish counted by the ROV to the distance from the edge of schools (as identified by acoustics). The analysis extended upto 50 m from the school edge. 0 m represents counts within the school. See Table 3 for model selection. Note that *y*-axis scaling differs among plots.

exclusion zone into the exclusion zone, there is still a potential that non-schooling fish located within the exclusion zone are being missed. Because the BASSCam is only deployed in schools identified by the acoustics, and if no acoustically identified school above the exclusion zone exists, the acoustics cannot be extrapolated downwards to correct for these missed fish. In this study, the addition of ROV belt transects allowed us to estimate background density, the density of fish within the exclusion zone that are not associated with fish schools. Since we observed little difference in the background densities of our target species/species groups between reefs, we suggest a single background density correction could be considered for all survey areas. In future studies, utilizing either BASSCam or ROV derived background density data would allow for a full population estimate that corrects for these missed fish. As a co-occurring ROV survey and large-scale acoustic–visual survey is not feasible, it is possible that a fixed correction could be generated by ROV surveys conducted outside of the time frame of the acoustic–visual survey, or that the BASSCam could be deployed haphazardly along the transect and counts from the downward-facing camera used to generate a background density. A cheaper solution is to apply the background density data from this study, but would need to be done in association with the caveat that the potential for time varying densities is being ignored.

An important consideration with genera like *Sebastes* is the allocation of acoustic data to different species. Opportunely, our finding that demersal rockfish remained within 1 m of the bottom implies that despite the great diversity of rockfish in Oregon's nearshore, many of these species occur outside of the observational scope of the acoustics, and therefore do not contribute to our acoustic estimates or the resulting population estimate. As such, a potential contamination to our population estimate is only from 3 species (Canary (*S. pinniger*), Widow and Yellowtail Rockfish). The challenge of species differentiation is further simplified by the ease of detection of these species with the BASSCam. These non-focal semi-pelagic species have been shown to be good candidates for acoustic surveys (Stanley, 1999, 2000) and the methods we describe here could easily be adapted to continental shelf stocks.

A potential concern in using the BASSCam to provide species and length composition data to apportion backscattering data into density is that it creates point estimates from a limited number of fish schools on each transect, as opposed to species and length data from the entire length of the transect. As the ROV conducted belt transects, we were able to assess

**Table 4.** Background ROV density (individuals per 100 $m^2$) and *SD* at each reef for each species/functional group. Background densities were calculated for the entire region >35 m from the outside edge of schools observed in the acoustic sampling. Raw density: the mean transect density assessed by the ROV main camera; *SD*: the standard deviation of the raw density among transects; Adjusted density in exclusion zone: Raw density multiplied by the proportion of fish in the 0–1 m exclusion zone in the ROV's stereo cameras, out of the total fish within 2 m of the bottom; N: number of transects.

| Species | Reef | Raw density | *SD* | Adjusted density in exclusion zone | Adjusted *SD* | N |
|---|---|---|---|---|---|---|
| Black | Bandon | 0.193 | 0.317 | 0.141 | 0.233 | 17 |
| Black | Arago | 0.449 | 0.866 | 0.324 | 0.624 | 13 |
| Black | Orford Reef | 0.193 | 0.331 | 0.130 | 0.223 | 18 |
| Black | Redfish Rocks | 0.311 | 0.357 | 0.120 | 0.138 | 17 |
| **Black** | **All Reefs** | **0.275** | **0.487** | **0.170** | **0.301** | **65** |
| Blue/Deacon | Bandon | 0.123 | 0.362 | 0.070 | 0.207 | 17 |
| Blue/Deacon | Arago | 0.380 | 0.630 | 0.191 | 0.317 | 13 |
| Blue/Deacon | Orford Reef | 0.981 | 1.357 | 0.476 | 0.658 | 18 |
| Blue/Deacon | Redfish Rocks | 0.108 | 0.266 | 0.037 | 0.091 | 17 |
| **Blue/Deacon** | **All Reefs** | **0.408** | **0.867** | **0.197** | **0.418** | **65** |
| Demersal | Bandon | 0.289 | 0.299 | 0.278 | 0.288 | 17 |
| Demersal | Arago | 0.530 | 0.555 | 0.505 | 0.528 | 13 |
| Demersal | Orford Reef | 0.324 | 0.243 | 0.304 | 0.228 | 18 |
| Demersal | Redfish Rocks | 0.174 | 0.168 | 0.165 | 0.159 | 17 |
| **Demersal** | **All Reefs** | **0.317** | **0.343** | **0.300** | **0.325** | **65** |
| Non-Focal Semi-pelagic | Bandon | 0.550 | 1.832 | 0.523 | 1.742 | 17 |
| Non-Focal Semi-pelagic | Arago | 0.263 | 0.389 | 0.222 | 0.328 | 13 |
| Non-Focal Semi-pelagic | Orford Reef | 0.186 | 0.218 | 0.136 | 0.160 | 18 |
| Non-Focal Semi-pelagic | Redfish Rocks | 0.143 | 0.247 | 0.108 | 0.186 | 17 |
| **Non-Focal Semi-pelagic** | **All Reefs** | **0.285** | **0.961** | **0.228** | **0.766** | **65** |

whether our point estimates missed species and/or size classes of fish. There were few species only observed by one video tool and not the other. Where species were only observed by one tool, it was often the ROV observing non-rockfish species or demersal rockfish. The first were excluded from analyses based on the school detection algorithm because it is adjusted to look for schools known to be rockfish. The latter were excluded since, as discussed above, they are almost exclusively located in the exclusion zone. Therefore, we suggest point estimates from the BASSCam can provide valid assessments of species and length composition of acoustically-available species for a reef.

It is worth noting that the total number of fish counted by the ROV is much higher than the total for the BASSCam; however, since the conversion of acoustic backscattering data into density only requires the relative proportions of the species (where total abundance is not important), this has little effect. The length distribution observed by the ROV and BASSCam did not differ in most instances because the ROVs length data were taken from the entirety of the transect and the BASSCam from schools, this suggests that there is no size fractionation between schools and individuals not located within schools. Overall, these data suggest that point estimates taken within schools, by the BASSCam, provide accurate species and length composition data.

Density estimates for schooling target species/species groups derived from our video-hydroacoustics were much greater than those derived from ROV data. This result was expected based on the semi-pelagic position of many of these fish. Rasmuson *et al.* (2021) demonstrated there was strong coherence between the population estimate from a previous passively integrated transponder (PIT) tagging study, and combined video–hydroacoustic survey. Our work further confirms that this combined survey method is well designed for the target species/species groups in this study. Similar to the findings of Rooper *et al.* (2020), the choice of which video sampling tool is used depends on habitat and species. In our case, we find that the suspended stereo system is better designed to sample nearshore semi-pelagic fish than bottom oriented tools like benthic video landers and ROVs. Although some individuals of our focal species are present within the exclusion zone, most are located above it and therefore are readily observed by the acoustics and the BASSCam, as is shown by the much higher density of fish estimated by the acoustic–visual survey tool. Regardless, fish within the exclusion zone not observed by the acoustics (both schools and background densities), potentially could be corrected for using the downward-facing camera on the BASSCam. Advantageously, most of the non-focal species are located almost exclusively within the exclusion zone, so they do not contribute to the acoustic estimate. Regardless of the utility of the tools, it is important to note that the coefficient of variation values for both survey tools were high. This is likely because the transects were very short (300–500 m) which greatly contributed to increased variability in the data. Application of a combined hydroacoustic video survey to a full, regional-scale, population survey would require longer (multiple kilometers) transects, which would likely reduce the variance in the density estimate seen in the present study. Further, this study demonstrated strong spatial and temporal variability within and between reefs, suggesting that for both the ROV and acoustics, modelling-based approaches to population estimates are likely the best way forward.

While these methods are specifically designed for nearshore species, they can easily be adapted to work with semi-pelagic shelf rockfish stocks. Our work demonstrates that the exclusion zone does not negatively affect the ability of the tool to sample our target species/species groups. Using our

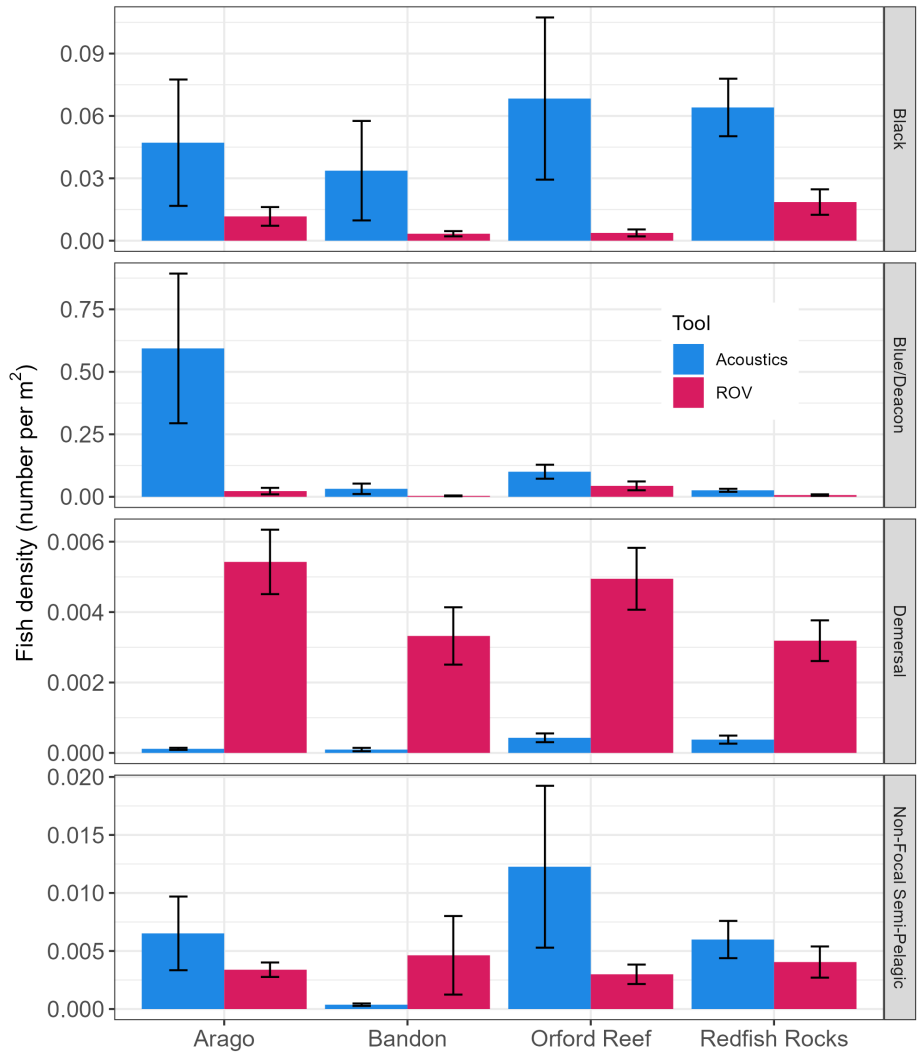


**Figure 7.** Mean reef-level density estimates from each of the 2 sampling tools for each reef and species group. Error bars denote *SD*. Acoustics- denotes densities generated from video–hydroacoustic combined sampling.

**Table 5.** Coefficient of variation for the density estimates for each of the species/species groups for each tool at each reef, and for all reefs on average.

| Reef | Black | | Blue/Deacon | | Non-focal semi-pelagic | | Demersal | |
|---|---|---|---|---|---|---|---|---|
| | Acoustics | ROV | Acoustics | ROV | Acoustics | ROV | Acoustics | ROV |
| Arago | 0.43 | 0.72 | 0.54 | 0.48 | 0.56 | 1.50 | 1.25 | 1.64 |
| Bandon | 0.39 | 0.74 | 0.42 | 0.63 | 1.06 | 0.37 | 0.62 | 1.13 |
| Orford Reef | 0.45 | 0.59 | 0.95 | 0.66 | 0.46 | 0.95 | 1.03 | 1.50 |
| Redfish Rocks | 1.28 | 0.84 | 1.37 | 0.65 | 1.12 | 0.83 | 0.99 | 1.53 |
| Average | 0.63 | 0.72 | 0.82 | 0.61 | 0.80 | 0.91 | 0.97 | 1.45 |

conservative exclusion zone (all areas within 1 m of the bottom) enhances the utility of the tool by reducing the number of species we observe. Ultimately, this ensures the acoustic density estimate primarily reflects target semi-pelagic rockfish and is not contaminated by demersal rockfish. Furthermore, targeting fish schools with an easily deployable stereo video system provides an accurate estimate of species composition and length data. In an area where the visibility is characteristically bad, the ability to first identify large schools with hydroacoustic equipment and then deploy cameras directly into these schools greatly increases the chance of collecting data. In short, we find that the combination of acoustics and suspended stereo cameras is an effective survey tool for semi-pelagic rockfish.

## Supplementary data

Supplementary material is available at the *ICESJMS* online version of the manuscript.

## Data availability statement

The data underlying this article will be shared on reasonable request to the corresponding author.

## Author's contributions

LR and SM contributed to the design and conception of the study. LK, SM, SF, MB, KL, and PR participated in the methodology, data collection, and data analysis. LR, SM, and KL drafted the original version of the manuscript. All authors contributed to revising the manuscript and approved the final draft.

## Conflict of interest

The authors have no conflicts of interest to declare.

## Funding

Funding for this project was made available from the NOAA Saltonstall-Kennedy grant programme grant number NA17NMF4270223.

## Acknowledgements

We thank Dave DeBelloy of the CPFV Enterprise and Bob Pedro of the RV Miss Linda for their assistance in this project. We thank Alison Whitman, Greg Krutzikowsky, and David Fox for their assistance in obtaining the grant funding, and Bill Miller and Steve Kupillas for survey implementation and video review.

## References

Allouche, O., Tsoar, A., and Kadmon, R. 2006. Assessing the accuracy of species distribution models: prevalence, kappa and the true skill statistic (TSS): assessing the accuracy of distribution models. Journal of Applied Ecology, 43: 1223–1232.

Balk, H., and Lindem, T. 2000. Improved fish detection in data from split-beam sonar. Aquatic Living Resources, 13: 297–303.

Barange, M. 1994. Acoustic identification, classification and structure of biological patchiness on the edge of the Agulhas Bank and its relation to frontal features. South African Journal of Marine Science, 14: 333–347.

Denney, C., Fields, R., Gleason, M., and Starr, R. 2017. Development of new methods for quantifying fish density using underwater stereo-video tools. Journal of Visualized Experiments,129:e56635.https://www.jove.com/video/56635/development-new-methods-for-quantifying-fish-density-using-underwater. (Accessed 14 August 2018).

Garner, S. B., Ahrens, R., Boswell, K. M., Campbell, M. D., Correa, D., Tarnecki, J. H., and Patterson, W. F. 2022. A multidisciplinary approach to estimating red snapper, *Lutjanus campechanus*, behavioral response to mobile camera and sonar sampling gears. Fisheries Research, 246: 106155.

Gauthier, S., and Rose, G. 2005. Diel vertical migration and shoaling heterogeneity in Atlantic redfish: effects on acoustic and bottom-trawl surveys. ICES Journal of Marine Science, 62: 75–85.

Haralabous, J. 1996. Artificial neural networks as a tool for species identification of fish schools. ICES Journal of Marine Science, 53: 173–180.

Hilborn, R., and Walters, C. J. 1992. Quantitative Fisheries Stock Assessment: Choice, Dynamics and Uncertaincy. Chapman and Hall, New York (NY).

ICES. 2000. Report on Echo Trace Classification. ICES. http://www.ices.dk/sites/pub/Publication Reports/Forms/DispForm.aspx?ID = 35681 (Accessed 9 September 2020).

Jones, D. T., Wilson, C. D., De Robertis, A., Rooper, C. N., Weber, T. C., and Butler, J. L. 2012. Evaluation of rockfish abundance in untrawlable habitat: combining acoustic and complementary sampling tools. Fishery Bulletin, 110: 332–343.

Kloser, R. 1996. Improved precision of acoustic surveys of benthopelagic fish by means of a deep-towed transducer. ICES Journal of Marine Science, 53: 407–413.

Kloser, R. J. Fisheries Research & Development Corporation (Australia), CSIRO (Australia), and Marine Research. 2002. Development and application of a combined industry/scientific acoustic survey of orange roughy in the eastern zone. Fisheries Research and Development Corp. : CSIRO Marine Research, Hobart, Tasmania. Available at: https://www.frdc.com.au/sites/default/files/products/1999-111-DLD.pdf.

Kotwicki, S., Lauth, R. R., Williams, K., and Goodman, S. E. 2017. Selectivity ratio: a useful tool for comparing size selectivity of multiple survey gears. Fisheries Research, 191: 76–86.

Kotwicki, S., Ressler, P. H., Ianelli, J. N., Punt, A. E., and Horne, J. K. 2018. Combining data from bottom-trawl and acoustic-trawl surveys to estimate an index of abundance for semipelagic species. Canadian Journal of Fisheries and Aquatic Sciences, 75: 60–71.

Laidig, T. E., Krigsman, L. M., and Yoklavich, M. M. 2013. Reactions of fishes to two underwater survey tools, a manned submersible and a remotely operated vehicle. Fishery Bulletin, 111:54–67. http://fisherybulletin.nmfs.noaa.gov/1111/laidig.pdf. (Accessed 19 April 2018).

Love, M. S., Yoklavich, M. M., and Thorsteinson, L. 2002. The Rockfishes of the Northeast Pacific. University of California Press, Northridge, California (CA). 404pp.

McClatchie, S., Thorne, R. E., Grimes, P., and Hanchet, S. 2000. Ground truth and target identification for fisheries acoustics. Fisheries Research, 47: 173–191.

Mcquinn, I., Simard, Y., Stroud, T., Beaulieu, J., and Walsh, S. 2005. An adaptive, integrated 'acoustic-trawl' survey design for Atlantic cod (*Gadus morhua*) with estimation of the acoustic and trawl dead zones. ICES Journal of Marine Science, 62: 93–106.

Mello, L. G. S., and Rose, G. A. 2009. The acoustic dead zone: theoretical vs. empirical estimates, and its effect on density measurements of semi-demersal fish. ICES Journal of Marine Science, 66: 1364–1369.

Misund, O. A. 1997. Underwater acoustics in marine fisheries and fisheries research. Reviews in Fish Biology and Fisheries, 7: 1–34.

Nero, R. W., and Magnuson, J. J. 1989. Characterization of patches along transects using high-resolution 70-kHz integrated acoustic data. Canadian Journal of Fisheries and Aquatic Sciences, 46: 2056–2064.

Ona, E., and Mitson, R. B. 1996. Acoustic sampling and signal processing near the seabed: the deadzone revisited. ICES Journal of Marine Science, 53: 677–690.

R Core Team. 2020. R: A language and environment for statistical computing. R Foundation for statistical computing, Vienna, Austria. URL https://www.R-project.org.

Rasmuson, L. 2021. Susceptibility of five species of rockfish (*Sebastes* spp.) to different survey gears inferred from high resolution behavioral data. Science Bulletin, 2021–2025. Oregon Department of FIsh and Wildlife, Salem, Oregon (OR).

Rasmuson, L. K., Fields, S. A., Blume, M. T. O., Lawrence, K. A., and Rankin, P. S. 2022. Combined video–hydroacoustic survey of nearshore semi-pelagic rockfish in untrawlable habitats. ICES Journal of Marine Science, 79: 110–116.

Rooper, C. N., Williams, K., Towler, R. H., Wilborn, R., and Goddard, P. 2020. Estimating habitat-specific abundance and behavior of several groundfishes using stationary stereo still cameras in the southern California bight. Fisheries Research, 224: 105443.

Ryer, C., Stoner, A., Iseri, P., and Spencer, M. 2009. Effects of simulated underwater vehicle lighting on fish behavior. Marine Ecology Progress Series, 391: 97–106.

Sawada, K., Furusawa, M., and Williamson, N. J. 1993. Conditions for the precise measurement of fish target strength *in situ*. The Journal of the Marine Acoustics Society of Japan, 20: 73–79.

Somerton, D. A., Williams, K., and Campbell, M. D. 2017. Quantifying the behavior of fish in response to a moving camera vehicle by using benthic stereo cameras and target tracking. Fishery Bulletin, 115: 343–354.

Stanley, R. 2000. Estimation of a widow rockfish (*Sebastes entomelas*) shoal off British Columbia, Canada as a joint exercise between stock assessment staff and the fishing industry. ICES Journal of Marine Science, 57: 1035–1049.

Stanley, R. D. 1999. Diel vertical migration by yellowtail rockfish, *Sebastes flavidus*, and its impact on acoustic biomass estimation. Fish Bull,97:320–331.

Stoner, A. W., Ryer, C. H., Parker, S. J., Auster, P. J., and Wakefield, W. W. 2008. Evaluating the role of fish behavior in surveys conducted with underwater vehicles. Canadian Journal of Fisheries and Aquatic Sciences, 65: 1230–1243.

Totland, A., Johansen, G. O., Godø, O. R., Ona, E., and Torkelsen, T. 2009. Quantifying and reducing the surface blind zone and the seabed dead zone using new technology. ICES Journal of Marine Science, 66: 1370–1376.

Tschersich, P. 2015. Hydroacoustic survey of black rockfish abundance and distribution operational plan for the Afognak and northeast districts of the Kodiak management area, 2015. Alaska Department of Fish and Game, Division of Sport Fish, Research and Technical Services, https://wc.adfg.state.ak.us/static/regulations/regprocess/fisheriesboard/pdfs/2012-2013/ayk/fms12_07.pdf (Accessed 21 July 2017). Alaska Department of FIsh and Game, Division of Commercial Fisheries, Regional Operational Plan ROP. CF. 4 K.2015.18, Kodiak.

Tušer, M., Prchalová, M., Mrkvička, T., Frouzová, J., Čech, M., Peterka, J., Jůza, T., *et al.* 2013. A simple method to correct the results of acoustic surveys for fish hidden in the dead zone. Journal of Applied Ichthyology, 29: 358–363.

Visa, S., Ramsay, B., Ralescu, A., and Van Der Knapp, E. 2011. Confusion matrix-based feature selection.MAICS,710: 120–127.

Wood, S. 2006. Generalized Additive Models: An Introduction with R. CRC Press, Boca Raton, FL.

Wood, S. 2011. Fast stable REML and ML estimation of semiparametric GLMs. Journal of the Royal Statistical Society: Series B (Statistical Methodology), 73: 3–36.

*Handling Editor: Richard O'Driscoll*